Two dimensional boron nanosheets: synthesis, properties and applications

Jing Shang[a], Yandong Ma[b], Yuantong Gu[a] and Liangzhi Kou[a*]

[a]*School of Chemistry, Physics and Mechanical Engineering Faculty, Queensland University of Technology, Gardens Point Campus, QLD 4001, Brisbane, Australia*

[b] *School of Physics, State Key Laboratory of Crystal Materials, Shandong University, Shandanan Str. 27, Jinan 250100, People's Republic of China*

Liangzhi.kou@qut.edu.au

Two dimensional boron nanosheets have been proposed theoretically for a decade, but were experimentally synthesized until very recent time. Research into its fundamental properties and device applications has since seen exponential growth. In this Perspective, we reviewed recent research progress in 2D boron sheets, touching upon topics on fabrication, properties, and applications, as well as the discussions of challenges and future research directions. We highlight the intrinsically electronic, and mechanical properties of boron sheets resulting from their diverse structures. The facile fabrication and novel properties have inspired design and demonstration of new nanodevices; however, further progress relies on resolutions to technical obstructions like non-scalable fabrication techniques. We also briefly describe some feasible schemes that can address the challenges. It is expected that this fascinating material will offer tremendous opportunities for research and development for the foreseeable future.

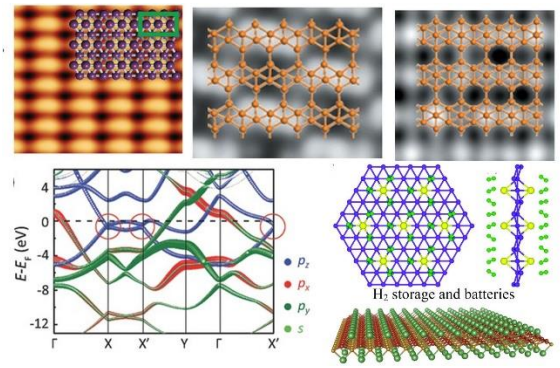

As a rising star material, boron nanosheets have been reviewed from the perspectives of synthesis, properties, application and possible research directions.

1. Introduction

The successful synthesis and revealed novel physics in graphene[1] have ignited the significant research enthusiasm of 2D layered materials due to the potential applications and outstanding performances.[2] Since then, hundreds of 2D materials, like graphene derivatives, g-C_3N_4, h-BN, layered transition metal dichalcogenides and Mxene [3-11] have been synthesized or proposed, they can exhibit insulating, semiconducting, metallic properties, even quantum spin Hall effect, superconductivity and multiferroics depending on the configurations and compositions, therefore potential used for spintronics, photovoltaics or quantum computation.[12] Among the 2D family, the mono-elemental counterpart which is composed with the elements at row IV and V attracted special research attentions due to the general presence of Dirac states, quantum spin Hall effects, high carrier mobility, and hexagonal sharps, including graphene, silicene, germanene, stanene, phosphorene, arsenene, antimone, bismuthene, [13-17] and also recently emerged atomic thick boron nanosheets.[18] The boron sheets (BSs) are the new members and were less investigated compared with widely studied graphene or phosphorene. One of the main reasons is that, boron is a special element, which is locating between metal Be and non-metal C in the periodic table, see Fig. 1f. The out-shell electron configuration of boron as the fifth element has only three valence electrons with the ground-state configuration of $2s^2 2p^1$, whereas it has four available valence orbitals achieved by promoting an electron from the 2s to the 2p orbital. The more usable atomic orbitals than number of electrons prevents the fulfilment of the octet rule, resulting in the electron-deficiency of the boron atom. As a result, 2D hexagonal (graphene-like) boron layers are unstable, since there are not enough electrons in the boron atom to fill all electron orbitals in a chemical bond based on the classic two-centre two-electron (2c-2e) bonds as in carbon systems.

Even so, the revealed diverse polymorphism of the boron nanosheets and the planar or semi-planar boron clusters in recent years demonstrated the presence of 2D BSs. It has been shown that the planar boron cluster can be stabilized by electron-surplus substrates or balanced by the vacancies. From theoretical simulations, the artificially built models based on the planar clusters[19] and structural search[20] made great contributions for clarifying the stable configurations of BSs, possible stabilization mechanism,[21] mechanical/electronic properties and feasible growth substrates. These pioneering works partially lead to the successful synthesis of BSs on the Ag or Al substrates, [22, 23] several different atomic thick BSs have been synthesized until now, see Figure 1a-1d. Vice versa, the successful experimental fabrication of the atomic thick BSs also greatly speeded up the fundamental researches and studies of potential applications, lots of novel properties have been revealed accordingly, promising applications have been proposed since. As an evidence of booming research interests, the publications related with BSs have shown an exponential increase from 2010, see Fig. 1f. However, the research output of plane boron is still much lower than that of graphene or MoS_2, indicating that the investigation for BSs is still in the infant period and there is a large unexplored space. In the review, we will firstly summarize the most important progress of planar boron clusters which can act as the precursors for 2D BSs. We then

review the theoretical proposed 2D boron layers, the possible stabilization mechanism and theoretically suggested synthesis methods. The latest progress of experimental fabrications of BSs will be also presented. Finally, we will review the basic mechanical and electronic properties of different BSs, and potential applications. The outlook and perspectives will be also briefly discussed. It is expected that the review can give a comprehensive and latest picture of BSs about fabrication, properties and applications.

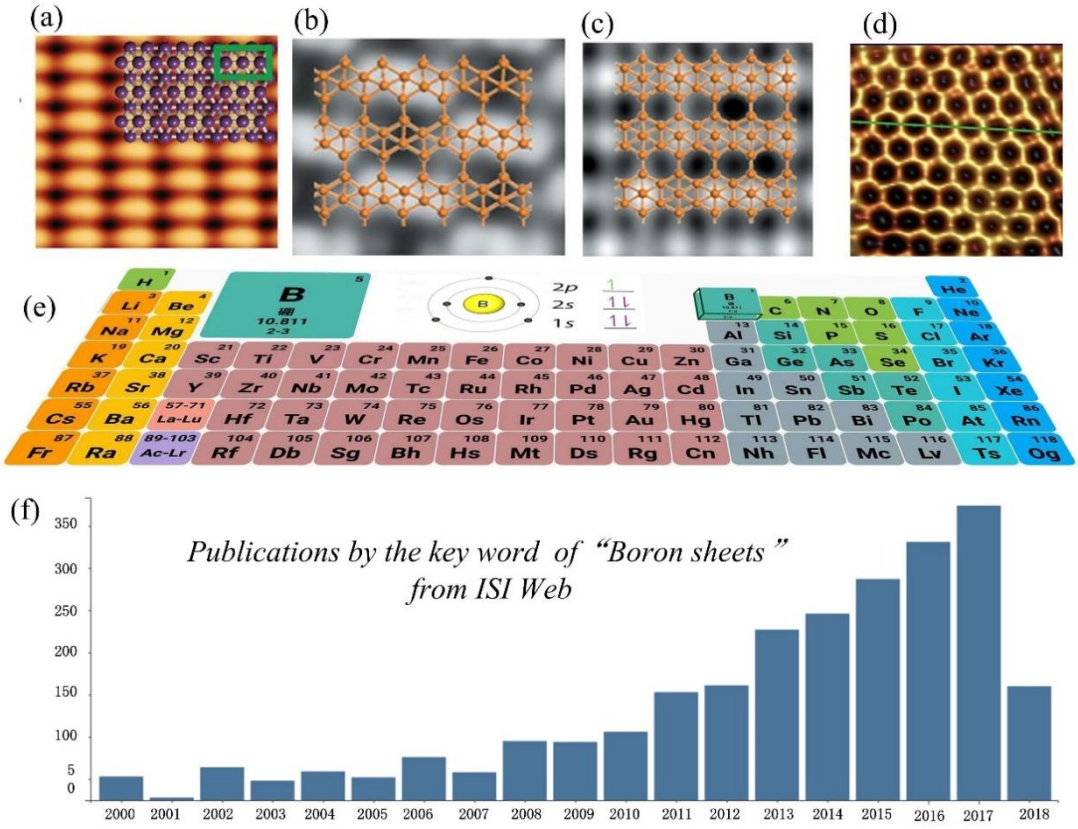

Figure 1. Four synthesized atomic thick BSs. (a) Triangular borophene on Ag (111) surface; Adapted with permission from ref. 8. Copyright 2015 The American Association for the Advancement of Science; (b) χ_3 sheet on Ag (111) surface; (c) β_{12} sheet on Ag (111) surface; ref. 9. Copyright 2016 Springer Nature; (d)[24] graphene-like BS on Al substrate; (e) the location of boron at Periodic table of element and the electron shell. Copyright 2018 Elsevier. (f) Summarized publications of boron sheets obtained from ISI web.

2. Planar Boron Clusters

Boron clusters were the most extensive research topics for decades[25,26] due to the possible applications in catalysis and drug design,[27] it is interesting to note that some of them exhibit planar structures as theoretically suggested and experimentally observed. These planar boron clusters were regarded as the precursor and can be used to build periodic 2D BSs, it is therefore essential to have a brief overview before going to 2D BSs, the clarifications of the ground states and atomic configurations of planar boron clusters will be helpful for explorations for 2D boron structures and the synthesis. Boron clusters we

discussed here refer to the 0D nanostructures with atom numbers less than 100, including small boron fragments or boron cages/fullerenes. As the topic here is about 2D BSs, we will mainly focus on the planar boron clusters. The smallest born cluster contains only 7 atoms (B_7), the global minima is a pyramidal planar configuration with one boron atom located at the centre of hexagonal shape as identified from photoelectron spectroscopy and ab initio calculations.[28] The cluster B_7 was then proposed as the building element of theoretically revealed triangular BSs (see the inset of Fig. 3e) and also experimentally synthesized borophene (see Fig. 1a and inset of Fig. 5a) as discussed following. When the atom number of cluster is increased to 10~15, the planar configurations of B_x clusters can still be well preserved as demonstrated by Zhai et al, see Fig. 2a. The planarity of all the boron clusters has been confirmed by the direct experimental evidences.[29] It is worthy to notice that all the clusters with the boron atoms up to 15 are composed with compact triangular lattice, no hexagonal lattice is included. The critical size of boron clusters which can maintain the planar configurations was then studied by from Kiran et al[30]. When the atom number exceeds 18, the 1D tubular structures which has a double-ring tubular structure with a diameter of 5.2 Å will be formed, see Fig. 2b. However, the ground states can be changed when external electrons are introduced. For example, it has been shown that the tubular structure of B_{20}^- anion is shown to be isoenergetic to 2D structures. Except the charge doping, the introduction of hollow hexagonal (HH) vacancies also effectively stabilizes the structures of planar boron cluster. For instance, B_{36} is a highly stable quasiplanar boron cluster when introducing a central hexagonal hole at the middle site (Fig. 2c), providing the experimental evidence that large size monolayer BSs with hexagonal vacancies are potentially viable.[31] The fullerene-like cage of B_{40} is the most stable configuration in the neutral state. However, the ground state is changed as a quasi-planar isomer when an external electron and two adjacent hexagonal holes are introduced[26] see Fig. 2d. For the larger boron cluster, higher densities and uniformly distributed HHs can further significantly reduce the total energies which render the planar or quasi-planar structures as the ground state. B_{56}, B_{70}, B_{84}, B_{98}, B_{112} and B_{120} clusters exhibit prefect planarity when 2, 3, 5, 6, and 7 HHs are introduced and uniformly distributed respectively,[32] although they were generally believed to prefer fullerene-like cages such as B_{40} and B_{80} buckyball [26, 33] or the core-shell like structure due to much higher energies in B_{80} fullerene cage as predicted by previous researchers. [34, 35] The introduction of HHs in the boron clusters well stabilizes the structures by balance 2c-2e bonds and 3c-2e (three-center, two-electron) bonds, therefore largely decreasing the binding energies, see Fig. 2e.

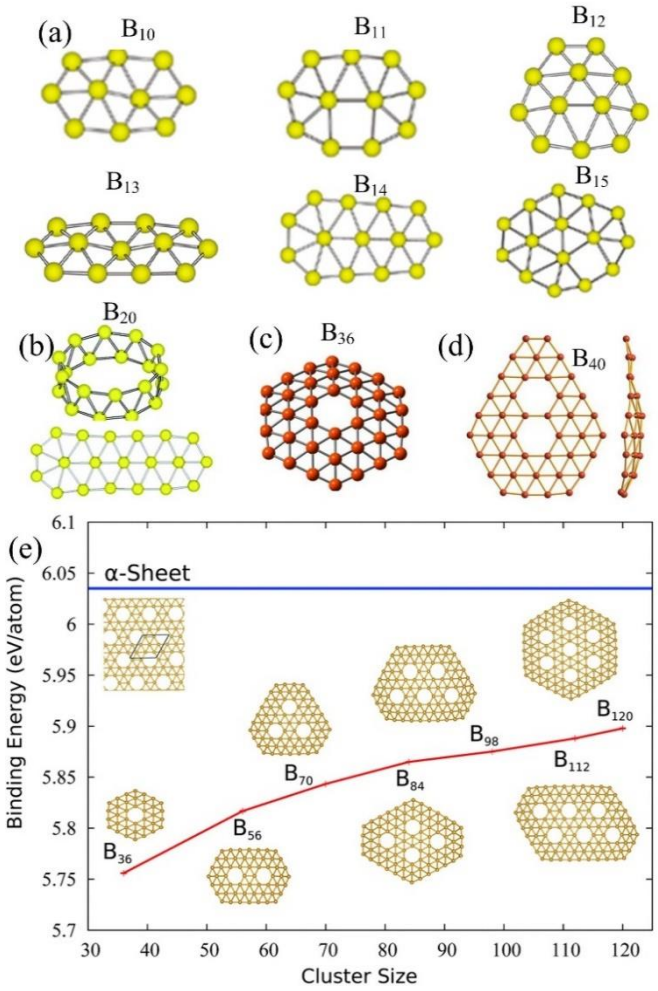

Figure 2. The planar boron clusters. (a) The stable configurations of planar B_x (x=10-15) clusters; Reproduced with permission from ref. 16. Copyright 2003 Springer Nature; (b) Tubular and planar B_{20} cluster; Ref. 17. Copyright 2004 Proceedings of the National Academy of Sciences of the United States of America; (c) Stabilized B_{36} with HH introduction, (d) HH and charge stabilized B_{40}-, ref. 20 and 13. Copyright 2014 Springer Nature; ref. 21. (e) The binding energies and atomic configurations of B_{36}-B_{120}, which are stabilized by the uniformly distributed HHs Copyright 2015 Royal Society of Chemistry.

The concise review of boron clusters including the key milestones revealed the importance of HHs density and charge states to maintain the planarity of boron nanostructures. These two factors can not only help to maintain the planarity to prevent forming bulk configurations, but also stabilize the structure by reducing the formation energy, therefore providing useful information about possible synthetic approach of the 2D BSs. The corresponding BSs with well-controlled HH densities are thus expected to be fabricated on some carefully chosen substrates which can donate the electrons.

3. Theoretical studies for structure searches and synthesis

Based on the planar stable boron clusters, the corresponding 2D BSs have been theoretically proposed, mostly based on first-principle calculations with PBE function, whose suitability for studying boron

materials has been validated. [36] The early concept about BS was motivated by the well-known layered AlB_2 phase, which is a puckered hexagonal system, all Al atoms are situated halfway between two flat honeycomb-shaped layers composed of B atoms.[37] The pure BSs can be obtained when the Al is removed and replaced with a boron, they exhibit buckled hexagonal sharps and compose with B_7 hexagonal pyramids in virtue of the Aufbau principle, see inset of Fig. 3a. The buckling of the triangular BSs along the out-plane direction is helpful for structural stabilization,[38, 39] it is a metal due to the electron deficiency[37, 40].

As indicated in boron clusters, the presence of HHs can remarkably stabilize the quasi-plane structures, the idea can be generalized to the corresponding 2D systems. As the successful examples, two flat BSs were predicted by Tang and Ismail-Beigi[21], which can be obtained by removing B atoms from a flat triangular sheet to create uniform distributed hollows, see Fig. 3a-3b. These obtained new sheets are composed of hexagons and triangles mixtures, which are metallic, flat, and more stable than the buckled triangular sheet by 0.12 and 0.08 eV per atom respectively. The stabilization mechanism is the same as large size boron clusters,[32] contributing to the competition between two-center bonding and three-center bonding. The B atoms at the hexagonal centre serve as the donors while the HHs act as the acceptors, they are mixed to compensate the electron deficiency, and stabilize the 2D structures. In the pioneering work, the dependence of binding energies on HH density was also studied. From the energetic calculations, the binding energies reach the maximum when the HH density $\eta \approx 1/9$ (defined as the ratio of hexagonal hollow number vs atom numbers in original triangular sheet). Taking the buckled triangular sheets as the reference, only the 2D boron layers within densities of $\eta = 0.1 \sim 0.15$ can be stabilized by the uniformly distributed HHs, the conclusion was confirmed by subsequent theoretical and recent experimental investigations. [22, 23, 41, 42]

The stabilization mechanism of 3c-2e and 2c-2e competitions induced by HHs pointed out the direction of predicting 2D BSs, namely the selective removal of B atoms from a close-packed triangular boron layer to produce hexagonal voids or vacancies. However, the strategy leads to a very large number of possible configurations, exploring which possesses a daunting combinatorial problem and hampers the direct use of first-principles methods. Hence, only a handful of BSs have been proposed and evaluated by density-functional theory (DFT) calculations. To solve the problem, Yakobson and co-workers[41] developed a new approach to study the structural diversity and stability of BSs based on the cluster expansion method, where the vacancies were treated as doped elements while the BSs containing HHs are regarded as pseudoalloys, which provided a thorough exploration of the possible configurations. As a result, a number of 2D stable polymorphs with nearly identical cohesive energies were discovered. Distinctly different in structure, they all lie in the rather narrow range of vacancy concentrations of 10-15%, which is well consistent with the findings by Tang and Ismail-Beigi.[21] Especially it was found that the formation energies of the BSs with $\eta \approx 1/9$, 1/8 and 2/15 are located at the bottle minimum area, indicating their high structural stabilities and feasibilities of experimental synthesis.

Except the DFT calculations, the direct structural search based on Particle Swarm Optimization method can locate the global structural minimum. The significant feature of this method is capable to predict both the ground and metastable structures with only the knowledge of the given chemical composition. Based on the particle-swarm optimization global algorithm, Zeng et al[20] predicted 16 boron monolayers with different HH densities η (0~1/3), two of them (α_1- and β_1-sheet) were filtered as the most stable α- and β-types BSs (η=1/8, Fig. 3c-3d), respectively. Both the sheets possess greater cohesive energies than the state-of-the-art 2D α-sheet[21] (by more than 60 meV/atom based on density functional theory calculation using PBE0 hybrid functional), as well as the η=1/8 and η=2/15 sheets (both belonging to the β-type)[41].

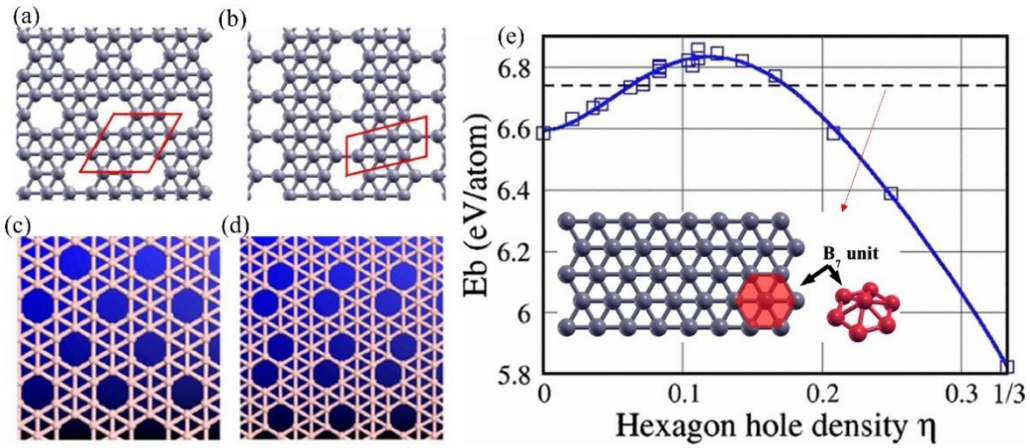

Figure 3. (a) Atomic configuration of α sheet with η=1/9; (b) the structure of β sheet with η=1/7; (c-d) α_1- and β_1-sheets with η=1/8; (e) Binding energies of BSs as a function of HH density η; the inset are the triangular borophene with η=0, and the smallest building unit B_7. Taken the binding energy of borophene as the reference, the stable BSs should have the HH density η=10~15%, while the most stable sheet corresponds to α sheet with η=1/9. Reprinted with permission from ref. 7. Copyright 2007 American Physical Society; ref. 6. Copyright 2012 American Chemical Society.

Different from 2D materials as graphene,[43] MoS_2,[8] phosphorene,[44] the experimental synthesis for BSs was almost absent before 2015. However, the theoretical researches provided some guidelines about the possible synthesis substrates and approaches. A dedicated chosen substrate is critical for experimental synthesis, the surplus electrons of substrates can be transferred to compensate the deficiency and thus stabilize the structures. First principles calculations suggested[45] that the metal surfaces (Mg, Al, Ti, Au, and Ag) can well stabilize the BSs as a result of electron compensation, the unstable hexagonal graphene-like sheet on the substrate is more energy-favourable than triangular or mixed hexagonal-triangular BSs. The findings indicate the importance and necessity of careful choosing metal substrates to synthesize the targeted BSs. It is worthy to point out that the theoretical prediction has been verified by recent experiments, graphene-like honeycomb planar BS has been synthesized on Al substrate.[24]

Following the ideas of CVD growth of graphene on Cu (111) surface,[46-49] the stability and growth mechanism of various BSs on Cu(111) substrate were also explored from theoretical simulations.[50] 2D planar boron cluster can continuously grow on the Cu (111) surface since the formation energy of planar boron cluster is linearly decreased with increasing cluster size, while the diffusion barrier for a single B atom is quite low. During growth process, hexagonal holes can easily arise at the edge of a 2D triangular boron cluster and then diffuse inwards. Hence, large-scale boron monolayer with mixed hexagonal-triangular geometry can be obtained via direct deposition of boron atoms. Except Cu surface, BSs can be also formed on other metal substrates (Ag, Au 111 surface) and metal boride (MgB_2, TiB_2) by atom deposition.[51] Driven by the gradient of the chemical potential, B atoms will assemble into 2D clusters first and further grow into a larger sheet, while formation of 3D boron structures is impeded owing to a high nucleation barrier. In addition, saturation of a boron-terminated MgB_2 surface in a boron-rich environment can also lead to the formation of B sheets. These sheets are weakly bound to the substrates, suggesting a feasible post-synthetic separation into the free-standing forms. For the possible BS growth on the Ag substrate, the micro nucleation mechanism of boron atoms on Ag surface was illuminated theoretically as in Fig. 4.[52] Small B clusters (B_{1-3}) would penetrate the first layer, but triangular fragments will gradually form on the Ag surface, and the hexagonal vacancies appear as the cluster size increases, see Fig. 4a. Because of the strong B-Ag interaction, the B clusters with the zigzag edge are stabilized, and that with vacancies in a stripe pattern would form through the probable diffusion of B atoms. It was concluded that the BS on the Ag (111) surface should contain 1/6 vacancies in a stripe pattern, since it is more energetically preferable. The findings are well consistent with the predictions from Zhang et al[53] where they employed the cluster expansion method to demonstrate that a planar $\eta_{1/6}$-sheet is favourable on the reactive substrates of Ag, Cu and Ni, Fig. 4b-4d. Most interestingly, these theoretical predictions have been verified by the subsequent experimental synthesis on the Ag (111) surface.[23]

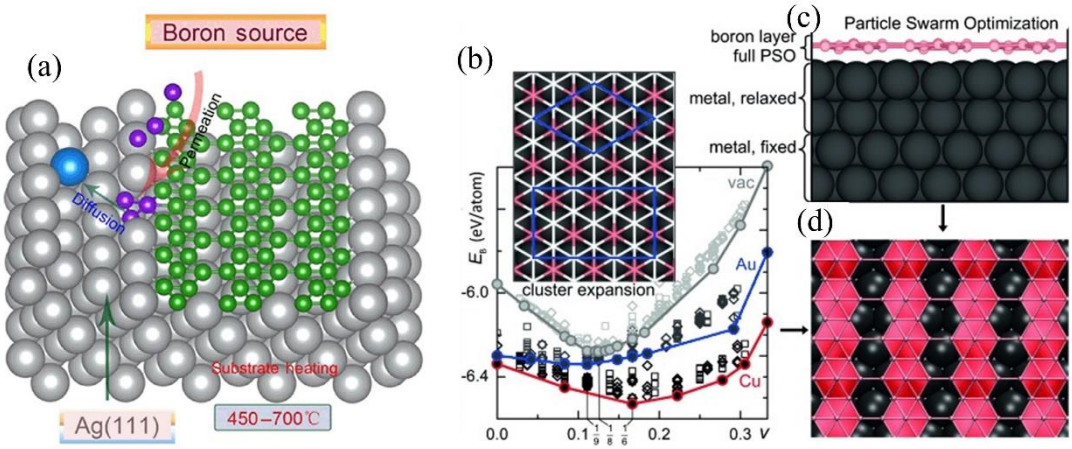

Figure 4. Theoretical proposed BSs growth on the substrates. (a) Theoretically proposed schematic diagram of η=1/6 BS growth on top of Ag (111) surface; (b) Total energy per atom of BSs with different HHs in the vacuum and on top of substrates of Au or Cu, the interaction between BSs and substrate was

included. (c) The BS-substrate model. (d) The predicted ground structures of β_{12} sheet with η=1/6 from theoretical simulation on Ag substrate. Reproduced with permission from ref. 35. Copyright 2016 Springer Nature; ref. 36. Copyright 2015 John Wiley and Sons.

These 2D BSs, regardless of artificially models or these from structural search, confirmed that the BSs with HH of 10~15% are energetically favourable. These theoretical investigations of possible synthesis have emphasized the importance of substrates and revealed metal substrate-dependent BS growth, therefore opening the possibilities to guide 2D boron formation through tailored boron-metal interaction and pave the ways for experimental synthesizing BSs on metal substrates and thus enrich the variety of 2D monolayer materials.

4. Experimental synthesis of BSs

The presence of planar clusters and the theoretical revealed stable 2D BSs indicate the promising possibilities of experimental synthesis, which have been confirmed by recent progresses. Under ultrahigh-vacuum conditions, Mannix et al[22] have shown that atomic thin crystalline 2D BSs with striped and close-packed triangular lattices (named as borophene, it will refers to the 2D buckled BS with η=0 in the following) can be synthesized on top of silver surface by MBE growth, which directly verified the proposed BSs from previous theoretical predictions.[38, 39] The atomically thin borophene was grown under the temperature of 550 °C (Fig. 5a) using a high pure solid boron atomic source to avoid the difficulties posed by toxic precursors, and ultrahigh vacuum conditions were required to avoid oxidation or contaminations. An atomically clean Ag (111) substrate provided a well-defined and inert surface for borophene growth. Scanning tunneling microscopy (STM) images demonstrated the emergence of planar structures exhibiting anisotropic corrugation (Fig. 5b), which was then confirmed from first-principles structure prediction. The atomically planarity of the BS was further verified via a suite of characterization techniques. The successful synthesis of borophene not only experimentally demonstrated the presence of atomic thick BSs for the first time, but also showed the power of theoretic simulations. The supports and mutual verifications from theory and experiments move the research area forwards.

Subsequently, another independent group confirmed the presence of 2D BSs. From MBE epitaxial methods, Wu et al synthesized two distinct boron layers on the Ag (111) surface, which were defined as S1 and S2 phases.[23] They have shown that the BS growth strongly depends on the temperature of Ag substrate. When it is lower than 570 K, only clusters and disordered boron fragments were obtained. However, the atomic island can be formed at around 570 K which will extend and cover the entire Ag (111) surface as the boron coverage is increased. Revealed from the high resolution STM images, the ordered parallel strip which is composed with 3Å×5Å rectangle lattice is S1 phase (Fig. 5c-5d). When the substrate temperature is increased to 680 K, a new phase of BS S2 can be obtained, the high resolution STM revealed the lattice difference, the distance between nearest neighbour protrusions

of S2 boron sheet are 3.0 Å along the rows and 4.3 Å across the rows (Fie. 5f-5f). Combined with first principles simulations (simulated STM images) and experimental observations, it was confirmed that the S1 phase corresponds to the theoretically predicted β_{12} boron sheets, while the unit cell of S2 shares the identical configurations of χ_3 sheets. Besides these two phases which cover most of the Ag (111) surface area, two metastable phases of 2D BS (named as S3 and S4) were also found on the substrate.[54] S3 phase shares the identical atomic structure of the previously reported S1 phase (β_{12} sheet) but has a different rotational relationship with the substrate, and thus exhibits very different features in STM images. The other new phase has a hexagonal symmetry and is proposed to be the long-sought α-sheet.

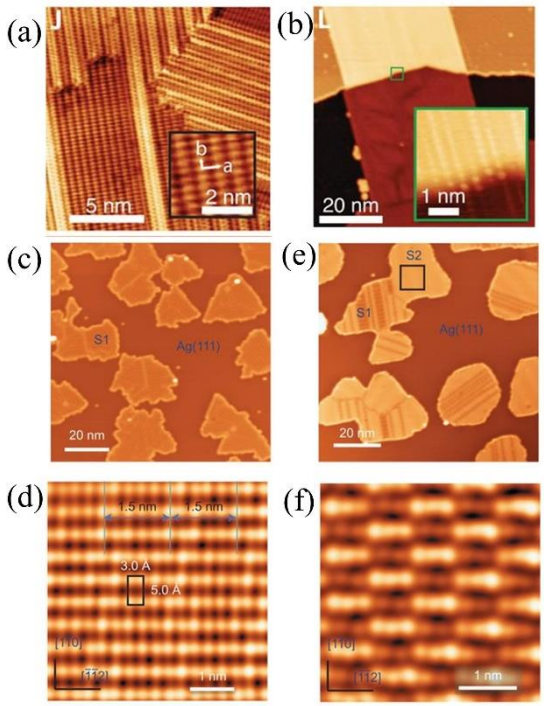

Figure 5. **Experimental synthesis of BSs**. (a) STM topography images showing striped-phase atomic-scale structure. Inset shows rectangular lattice with overlaid lattice vectors. (b) Striped-phase island and striped-phase nanoribbon. Inset shows atomic continuity across the Ag (111) step. Adapted with permission from ref. 8. Copyright 2015 The American Association for the Advancement of Science; (c) STM topographic image of boron structures on Ag (111), with a substrate temperature of ~570 K during growth. (d) High-resolution STM image of S1 phases. The S1 unit cell is marked by a black rectangle, and the 1.5 nm stripes are indicated by solid lines. (e), STM image of BSs after annealing the surface to 650 K. (f), High-resolution STM image of the S2 phase. ref. 9. Copyright 2016 Springer Nature;

Two independent groups have synthesized the BSs on top of Ag (111) surface, but the obtained configurations are distinct from each other, one is striped and triangular sheet with $\eta=0$[8], while the sheets from Wu's work[9] are mixed hexagonal-triangular boron sheets with $\eta=1/8$ or $1/9$. Controversial arguments were raised about the atomic configurations of BSs on Ag surface,[55] it was argued that the striped BSs found by Mannix et al is not the triangular lattice, but the S1 phase as revealed by Wu et al

in term of the rectangular lattice and STM images. The periodical corrugations for the strip phase are probable from nanoscale corrugations of the substrates, as revealed in a recent work by Zhang et al,[56] where periodic nanoscale one-dimensional undulations can be preferred in β_{12} BS on concertedly reconstructed Ag (111). This wavy configuration is more stable than its planar form on flat Ag (111) due to anisotropic high bending flexibility of the BS. However, the clarification about the atomic configuration on Ag surface requires more experimental evidences and further investigations as the structural difference probably comes from the different substrate temperatures during the synthesis (450-700 °C for Mannix one while 570-680 K for Wu et al).

Regardless of the controversies, the successful experimental synthesis of BSs, especially α sheet which was theoretically proposed to be the most stable, will not only greatly move the research area forward, but also validate the power of theoretical methodologies. The synthesized β_{12}, χ_3 and α boron sheets share one common feature, namely the presence of voids which mix 2c-2e and 3c-2e. Besides, the theoretical calculations also suggested the importance of electron transferring from substrate to stabilize BSs. The point has been proven by the graphene-like planar BS synthesis on Al substrate,[24] although they are strongly unstable at free-standing condition and heavily depend on the substrate. In contrast to the negligible charge transfer in case of borophene/Ag (111), one electron per born transferred from the Al (111) substrate significantly stabilizes the honeycomb structure. As a result, the BS will strongly bind with the substrate, and it is hard to peel off from the substrate.

Unlink traditional 2D layered materials, boron doesn't have a natural 3D allotrope with a layered structure, it is thus unsuitable to produce the 2D BSs with traditional mechanical exfoliation, but mainly depending on chemical method, like MBE growth. However, MBE methods encounter various drawbacks such as the need for ultra-high-vacuum/low-pressure growth, an additional transfer step that inevitably deteriorates the quality of the sheets, limited quantities, and insufficient yield, restricting their potential applications. Latest research indicates that high-quality few-layer BSs can be prepared in large quantities in dimethylformamide (DMF) and isopropyl alcohol (IPA) by sonication-assisted liquid-phase exfoliation,[57] the average area size can reach up to19827 and 1791 nm^2 at different liquid, with thickness of 1.8 to 4.7 nm respectively. In details, bulk boron powder with an average lateral particle size of 2 μm was firstly immersed into DMF/IPA and was sonicated at 350 W for 4 h. Then, the supernatant was centrifuged at 5000 rpm for 30 min to remove un-exfoliated B particles. Stable BS in both DMF and IPA were obtained for analysis. The obtained sheets have the advantages over these from chemical methods like the larger size, while the lateral size and thickness of the exfoliated sheets can be controllably tuned depending on the exfoliating solvent types and centrifugation speeds. Additionally, the exfoliated few-layer BSs exhibit excellent stability and outstanding dispersion in organic solvents without degradations for more than 50 days under ambient conditions, owing to the presence of a solvent residue shell on the sheet surface that provides excellent protection against air oxidation.

5. Physics, chemistry and mechanical properties

5.1 Electronic and transport properties

The successful synthesis has ignited the research enthusiasm of 2D BSs, novel mechanical and electronic properties have been revealed since. In contrast to the semiconducting or insulating properties in 3D bulk structures, most of the BSs are metallic. Taken the buckled borophene as an example,[22] the metallicity was revealed from accurate DFT calculations, the states from p_x, p_y and p_z orbits of boron cross the Fermi level along the Γ-X and Y-S directions, which are parallel to the uncorrugated direction. In contrast, the out-of-plane corrugation along another direction opens a band gap along the Γ-Y and S-X directions. As a result, borophene is a highly anisotropic metal, where electrical conductivity is confined along the chains. The anisotropic conductivity was proven by direct transmission calculation,[58] directional dependence of the transport properties in the BS was found, where the current along the chain direction is two times larger than that along out-of-plane corrugation.

Although it has been synthesized on the substrate, the freestanding borophene is slightly unstable as evidenced by the small imaginary frequency at Γ point (see supporting information of Ref. 8). The issue can be solved by functionalizing the surface using functional groups. Xu et al[59] suggested that full surface hydrogenation is an effective approach to stabilize the system where 0.715*e* is transferred from H to B to offset its electron deficiency. As a result, the imaginary frequency is removed and it is dynamically stable at 240 K. More interestingly, the hydrogenation removes the p_z orbit of boron from Fermi level, the states from the remained p_x and p_y orbits cross each other linearly to form Dirac cone with ultrahigh Fermi velocity. The stable hydrogenated BS exhibits novel mechanical features,[60] like ferroelasticity, negative Poisson's ratio, Dirac and transport direction switch under stain deformation, as well anisotropic conductivity,[58] therefore promising for interesting mechanical, and electronic device design.

The metallicity of β_{12} and χ_3 BSs was also confirmed from experimental measurements using angle-resolved photoemission spectroscopy (ARPES),[61, 23] the metallic states crossing Fermi level are mostly from p_z orbits of boron,[62] see Fig. 6a, which share some similarities with that of graphene. The π bands in graphene near the Fermi level (E_F), derived from the p_z orbital, form the Dirac cones at the K points. The similar phenomena is expected in these boron sheets. Recently, the simulation together with experimental investigations has proven the expectation in β_{12} sheets by Feng et al,[63] the periodic boron atoms in a honeycomb-like lattice can not only stabilize the structures by balancing out the two- and multicenter bonds, but also decompose the structure into two triangular sublattices (the one at the hexagonal center vanishes wave function at Fermi level owing to phase cancellation at the sixfold coordinated boron atoms), it is analogous to the honeycomb lattice of graphene, therefore hosts Dirac cones, see Fig. 6b. Due to the electron deficiency, the Dirac points were located at approximately 2 eV above the Fermi level, which is in good agreement with previous DFT report.[62] The Dirac cone has also been observed in ARPES experiment, but it is only located 0.25 eV below E_f. The difference between DFT calculations and

experiments is probably due to the presence of Ag substrate and unexpected doping effects, see Fig. 6c. Nevertheless, the direct experimental observation of Dirac cone provided the strong evidence for the theoretical predictions. Except β_{12} sheets, Dirac cone was also observed in χ_3 BS[64], see Fig. 6d-6e, it is anisotropic as observed from high-resolution ARPES. The survival of the Dirac cones is contributed to the weak hybridization between χ_3 sheet and Ag (111). As β_{12} and χ_3 sheets have been predicated to be superconductors, the results may stimulate further research interest in the novel physics of BSs, such as the interplay between Cooper pairs and the massless Dirac fermions.

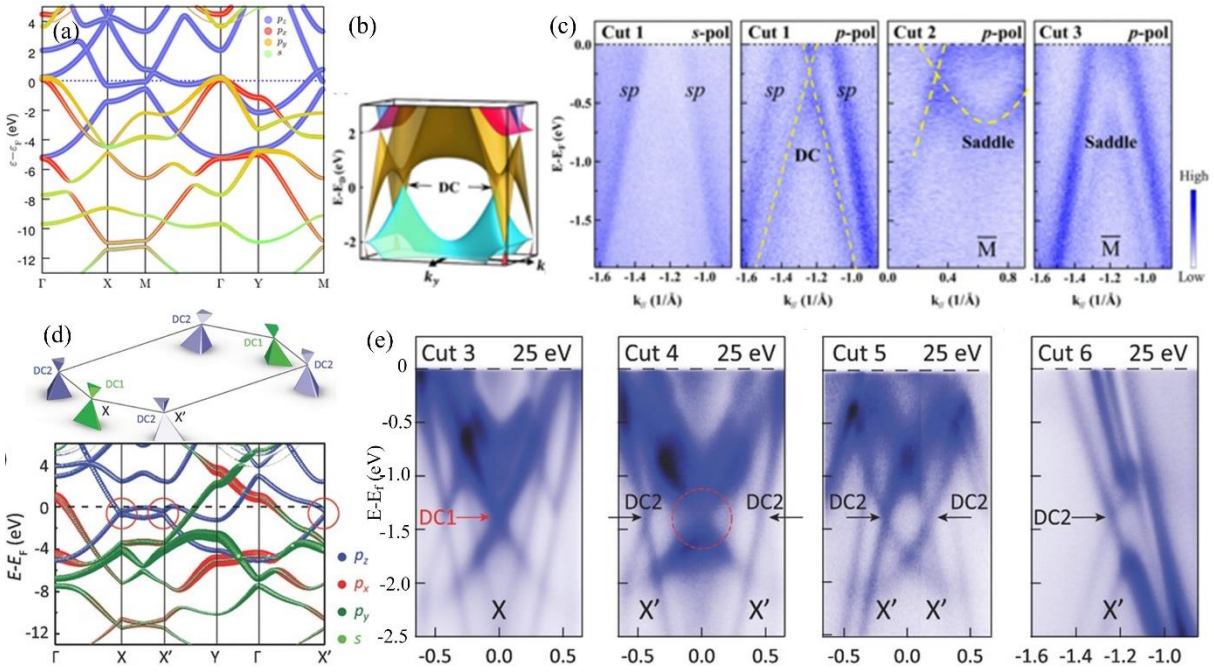

Figure 6. **The electronic properties and revealed Dirac cones in BSs**. (a) The orbit resolved bandstructure of β_{12} sheet with η=1/6, (b) 3D Band structures of free-standing β_{12} sheet. The black arrows indicate the Dirac cones. (c) ARPES intensity plot measured along cut 1 with *s* polarized light (first panel). ARPES intensity plots measured with *p* polarized light along cut 1 to cut 3, respectively. The yellow dashed lines indicate the Dirac cones. (d) Schematic drawing of the anisotropic Dirac cones in χ_3 sheet. Black lines indicate the Brillouin Zone. Orbit resolved band structures of free-standing χ_3 sheet are shown below. The Dirac cones are highlighted by the red circles. (e) ARPES intensity plots of χ_3 measured along cuts 3-6 with *p* polarized light. Red and black arrows indicate the Dirac cones at the X and X' points, respectively; Reproduced with permission from ref. 42. Copyright 2016 American Chemical Society; ref. 45. Copyright 2017 American Physical Society; ref. 46. Copyright 2018 John Wiley and Sons.

The Dirac feature is not unique in β_{12} and χ_3 BSs, it was also predicted theoretically in 2D Pmmn boron sheet,[65] graphene like ionic boron,[66] striped boron sheet[67] and boron hydride sheets,[68] but these were yet experimentally confirmed. Except the pure BSs, metal decorated boron layers also exhibit interesting electronic properties. Embedding a metal atom which can donate electrons to the boron framework not only stabilizes the structure, but also leads to the isoelectronic analogue of graphene as metal borides. For example, 2D monolayer TiB_2 sheet[69], which can be built as metal Ti occupies the hexagonal centre of honeycomb BS, was found to be characterized with anisotropic Dirac cones with the large Fermi velocity. Similar systems

include, MgB_2,[70, 71] BeB_2,[72, 73] FeB_2,[74] FeB_6[75] and β_{12}-$XBeB_5$ (X = H, F, Cl) derived from β_{12}-Borophene.[76] The chemical modifications based on revealed BSs have led to interesting electronic properties and possible applications.

5.2 Superconductivity

The metallicity in BSs and strong electron-phonon coupling strength in boron imply that pure boron layers are ideal candidates of superconductors. This expectation can be seen from monolayer MgB_2, the honeycomb boron layer combined with a layer of Mg on the hexagonal centre, it possesses the superconductivity at ~40 K[77] due to the strong electron-phonon coupling and intrinsic metallicity. The metallic bands of MgB_2 at the Fermi level, which is important for the superconductivity, mainly derive from B orbitals rather than the metal atoms.[78, 79] Remarkably, Zhao et al[80] proved the superconductivity in BSs from theoretical calculations, the conventional BCS superconductivity in the stable 2D boron structures is ubiquitous with the critical temperature Tc above the liquid hydrogen temperature for certain configurations. The superconductivity and critical temperature are sensitive to the detailed structures of the BSs, it shows a V-like function of HH density η,[81] see Fig. 7. Meanwhile, Penev et al[62] also studied the electron-phonon coupling strength and showed that 2D boron may be indeed a conventional superconductor with critical temperatures Tc ≈ 10-20 K, where Tc increases with decreasing density of HHs. The conclusion was proven in an alternative research work.[82] The electron-phonon coupling constants in β_{12} and χ_3 sheets, are even larger than that of MgB_2. The predicted critical temperatures (18.7 K and 24.7 K) are much higher than that of graphene (theoretically predicted 8.1 K[83] and experimentally observed 4.5 K superconductivity).[84] The mutual verifications from independent research groups indicate that 2D boron structure may be a mono-element material with the high Tc on conditions without high pressure and external strain. Moreover, the superconductivity is tunable with external field, which provided flexibility for superconducting device design. For example, Cheng et al[85] demonstrated that the superconductivity of substrate-supported β_{12} sheet can be supressed by tensile stain and electron doping. The 2% biaxial tensile strain induced by Ag (111) significantly reduces the superconducting transition temperature Tc of β_{12} sheet from 14 K to 2.95 K; 0.1e per boron atom electron doping further shrinks Tc to 0.09K. In contrast, it can be enhanced to 22.82 K with proper compressive strain (-1%) and 18.97 K with hole doping (0.1h+ per boron). The orbit analysis indicates that the variation of Tc is contributed to the density of states of σ bands near the Fermi surface. However, in an alternative work,[86] it has shown that the tensile strain can increase Tc from 19 to 27.4 K, the contradictory conclusion from different work indicates the necessity of deeper understanding for the external field effect on superconductivity. Even so, the conclusion that Tc increases with hole doping is consistent from these two works. Since the alkali metal adsorption on the surface can always lead to electron doping, the superconductivity should be also tuned accordingly. Wu et al[87] revealed that the superconducting Tc for Li-incorporated boron layers, Li_2B_7, is 6.2 K because of the small DOS at the Fermi level and electron doping. Overall the superconductivity has been clearly predicted in all BSs,

however it has not been unambiguously observed in experiment yet. One possible reason is the suppression of superconductivity induced by tensile strain and electron doping as indicated above.

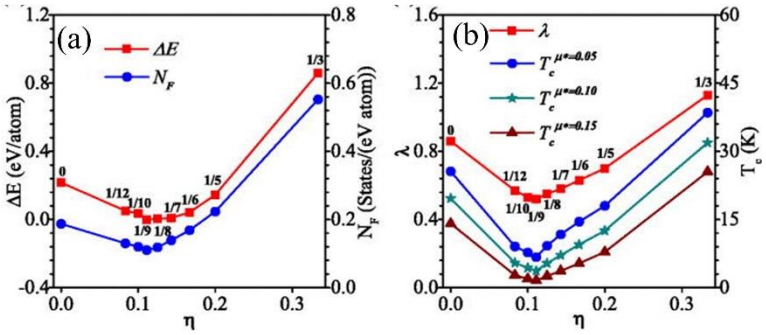

Figure 7. (a) Total energy and N_F (EDOS at) vs HH density η. The square (circle) line represents the total energy which is scaled by the left (right) rim of the graph. The total energy of the α-sheet is set to be zero. (b) electron-phonon coupling strength λ and critical temperature Tc vs η. The square (circle, star, and triangle) line represents λ which is scaled by the left (right) rim of the graph. Reproduced with permission from ref. 63. Copyright 2016 AIP Publishing.

5.3 Mechanical properties

Due to the presence of strong B-B valance bonding, BSs possess outstanding mechanical properties. From the experimental measurements,[22] the buckled borophene exhibits substantial mechanical anisotropy resulting from the unique structure. Owing to the strong, highly coordinated B-B bonds, the in-plane Young's modulus is equal to 170 GPa·nm along b direction, and 398 GPa·nm along a direction, which are well consistent with subsequent theoretical estimations (163 and 382 Gpa nm)[88]. The excellent mechanical feature potentially rivals graphene, at 340 GPa·nm.[89] More interestingly, it was found borophene possesses the negative in-plane Poisson's ratio (-0.04 along *a* and -0.02 along *b*) due to the unique out-of-plane buckling. The phenomena is preserved when the borophene is fully hydrogenated, but auxetic behavior is along the out-plane direction.[74] As a result of passivation, the mechanical stiffness of hydrogenated borophene (also named as borophane) is reduced, the in-plane Young's modulus reduces to 190 and 120 GPa nm along two different directions due to the weaken B-B bond length.[59] As discussed above, the introduced HHs in BSs can effectively stabilize the structures, they will also strongly affect the mechanical properties. It has been observed that the in-plane stiffness has an obvious dependence on the densities. For example, the in-plane Young's modulus of the BS with η=1/6 is 210 N/m and 190 N/m along and across the HH rows, and 205 N/m for BS with η=1/5. For the most stable α BS (η=1/9), the stiffness is almost isotropic with value of 214 N/m.[88] The stiffness of all the BSs is obviously smaller than that of buckled borophene. The reason is that the mechanical strength is dominated by the B-B bonding intensity as well as the B-B bonding number along the strain direction. The introduction of HH will obviously decrease the B-B bonding number, therefore weaken the stiffness. An alternative consequence of HH introduction in 2D boron lattices is, the ultimate tensile strength will be also greatly affected. The ultimate tensile strength for BSs along armchair direction is reduced from 22.8 Gpa nm (η=0)

to 19.97 Gpa nm (η=1/6) and 14.84 Gpa nm (η=1/9), however the strength along zigzag direction is slightly increased. Poisson's ratio and bending stiffness also showed strong dependence on the HH density, which indicates large flexibility of these mechanical parameters, therefore can meet diverse requirements for applications.[90]

5.4. Optical and chemical properties

5.4.1 Optical properties: Except these novel mechanical and electronic features, BSs also show interesting optical and conductivity properties. Adamska et al[91] found β_{12} and δ_6 BSs to be anisotropic metals, with strong energy- and thickness-dependent optical transparency and a weak absorbance in the visible range (less than 1%). A transition from transparent to reflective metallic behaviour can be induced in the visible for layered films, as the thickness is increased from ~1 nm in the monolayer to ~20-30 nm. They can therefore serve as a complement to graphene as a metallic monolayer that is transparent in the visible range.

5.4.2 Chemical stability: For most of the experimental synthesized BSs, they were chemically grown in an ultrahigh-vacuum condition to avoid the degradation and contaminations from environments. Although it was claimed that the BSs were inert to the oxidations where the region of prefect sheets keep intact under ambient condition for a period,[26] they can be still contaminated after long-time exposure to air[22] due to electron deficiency of boron atoms and relative high chemical activity of the surface. Recent theoretical investigations[92] showed that oxygen molecule can be spontaneously adsorbed on its χ_3 sheets in a manner of chemical adsorption, which will be dissociated after overcoming the energy barrier of ~0.35 eV. However, the dissociated O is difficult to move on the surface due to the strong B-O bonding and poor mobility at room temperature, ultimately leading to the boron oxides. The effect of substrate [Ag (111) surface] on the oxidization process was also studied for buckled triangular BSs.[85] The O_2 molecule on the free-standing borophene will have a triplet to singlet transition. However, such a spin transition does not take place upon the presence of the Ag (111) surface, the exothermic character of the borophene oxidation has been strengthened in comparison with the free-standing system. This can promote the formation of boron vacancies on the borophene sheet, giving rise to a somewhat planar structure on the Ag (111) surface.

As BSs can be easily oxidized, it would be a challenge to utilize the intrinsic outstanding mechanical and electronic properties of BSs in the ambient conditions. It is therefore essential to develop the packing techniques for fabricating air-stable BS based devices, like phosphorene.[44]

6 Applications

Although 2D BSs have been theoretically proposed for a long time while some novel properties have been revealed, they were only successfully experimentally demonstrated in very recent time. The possible applications are still in tentative explorations, the investigations along this direction are rare but highly promising. We here briefly review the recent BSs' applications, mainly focus on the energy

storages although they are also promising used in other area, like the enhanced electro-optical performances.[93]

6.1 Hydrogen storage

2D materials are perfect for hydrogen storage and gas sensing because of the large surface-volume ratio.[94] With the aid of transition metal or alkali metal adsorptions, Graphene,[95] MoS_2,[96] BN[97] and so on[98] have been proposed for the application purpose. Two main indexes have been used to assess the merits of hydrogen storages; 1: the adsorption energy, it should be in the range of 0.2-0.6 eV/H_2, so that H_2 molecules can be stably adsorbed on the surface while it is easy to desorb under thermal process; 2: H_2 adsorption capacities. BSs possess a couple of advantages over other 2D materials, first of all boron is the lightest element among the 2D material family, it is therefore potential to possess high gravimetric hydrogen density, secondly the intrinsic HHs in BSs can act as alkali/transition metal adsorption sites, it avoids to create defects to trap metals for hydrogen adsorption like graphene.[99]

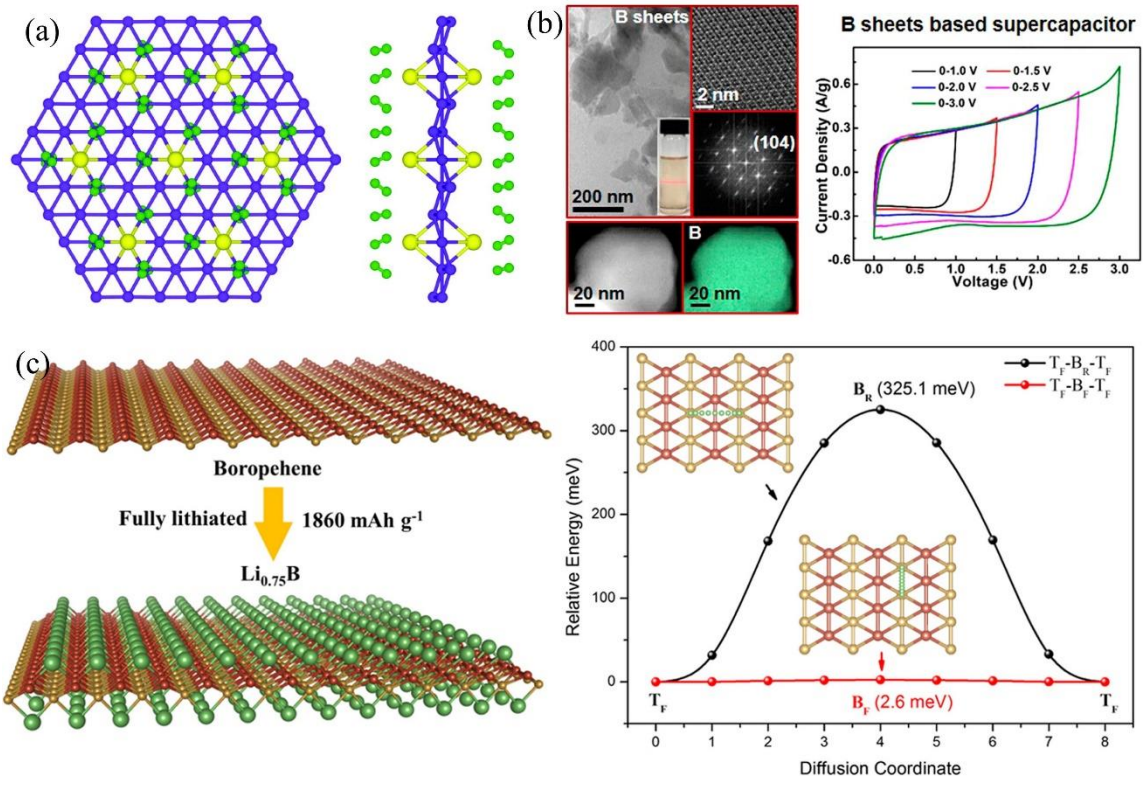

Figure 8. Summarized applications of boron nanosheets. (a) Hydrogen storage on alkali metal decorated α boron sheet. (b) Boron sheets produced by the exfoliation, and the measured performance of the supercapacitor based on them. (c) Buckled boron sheets as the Li ion batteries, and the corresponding diffusion barrier on the different directions. Reproduced with permission from refs. 19. Copyright 2009 American Chemical Society. Reproduced with permission from ref 57. Copyright 2018 American Chemical Society. Reproduced with permission from ref 106. Copyright 2016 Elsevier.

The recent work by Tang et al[100] proves these two points using β_{12} BS as an example, it was found β_{12} sheet is a perfect candidate for calcium-decoration and hydrogen storage application. In contrast to graphene where defects are required to capture Ca, the naturally formed HH ring in β_{12} BS provides the ideal site for Ca adsorption, and up to $6H_2$ molecules for each Ca atom can be captured with a desirable binding energy of ~0.2 eV/H_2. The gravimetric hydrogen density for Ca decorated BS can reach up to 8.92 wt%. For Ca-decorated χ_3 BSs, a comparable gravimetric hydrogen density can be also achieved, reach to 7.2 wt%.[101] From the electronic analysis, both the orbital hybridizations and polarization mechanism play significant roles in H_2 adsorption and storage. The gravimetric hydrogen density in BSs is comparable to that of graphene (~10 wt%).[95] The merit of hydrogen storage can be greatly improved when using lighter metal elements for decoration. Alkali metal decorated α boron R-sheet can physisorb up to a maximum of 10.7 wt % hydrogen. For buckled triangular BSs which is decorated with Li ions,[102] the hydrogen storage capacity reaches up to 13.7 wt% with an average adsorption energy of 0.142-0.176 eV/H_2. The lower adsorption energy is originated from the less electrons transferring from Li ions to hydrogen, which weaken the interaction between H_2 and BSs. At the room temperature, the hydrogen capacity is still up to 9.1 wt%. Several other theoretical investigations[103, 104] also conclude the similar conclusions, however the direct experimental verification is still absent.

Besides boron nanosheets, other boron nanostructures like fullerenes and nanotubes, were also proposed as the promising hydrogen storage media due to their relative active chemical activity of the surface. For example, Ca-coated boron fullerene (B_{80}) and nanotubes were theoretically demonstrated as excellent hydrogen storage materials. It was found that B_{80} fullerene and (9, 0) nanotube coated with 12 Ca atoms can store up to 60 H_2 molecules with an average binding energy of 0.12-0.40 eV/H_2 and 0.15eV/H_2, respectively, corresponding to a gravimetric density of 8.2 wt% and 7.6 wt%.[105] Different from the plane flat structure in 2D boron sheets, the surfaces of boron fullerene and nanotube are bended, the curvature probably affects the hydrogen adsorption, which is worthy for the further investigations.

6.2 Batteries and supercapacitor

The intrinsic HH in BSs can tightly hold the adsorbed metals, which not only facilitates H_2 storage, but also enhance the stability of the whole system, therefore promising for battery applications. Recent theoretical investigations[106] show that borophene is potential as an anode material for lithium-ion batteries. Lithium atom on borophene has an adsorption energy of -1.12 eV, which is large enough to ensure a good lithium-borophene stability during the lithiation process. The maximum adsorbed Li ion for each boron atom is up to 0.75 ($Li_{0.75}B$), corresponding to a theoretical specific capacity of 1860 $mAhg^{-1}$, it is about 4 times larger than that of the commercial graphite anode (372 $mAhg^{-1}$). More excitingly, lithium diffusion on borophene can be extremely fast as the energy barrier along the furrow of corrugated borophene is only 2.6 meV, it is much lower than those of other widely investigated anode materials such as phosphorene (80 meV) and Ti_3C_2 (70 meV). However, the energy barrier

perpendicular to the furrow of borophene is large as 325.1 meV, leading to much slower lithium diffusion along the direction. More importantly, borophene keeps metallic characteristics during the whole lithiation process, to ensure that the material has an excellent electronic conductivity. Alternative studies confirmed the conclusion on the battery performance.[107] Meanwhile, when the Li ion is replaced with Na, Mg, Al and Ca, borophene can still act as an excellent anode material with small diffusion barriers and large capacities.[108-111] Even it is fully hydrogenated, the outstanding battery performance is well preserved (large binding energy of Li/Na; small diffusion barrier;[112]), although the maximum theoretical specific capacity is significantly reduced to 504 mAh/g (but still larger than 372 mAh/g of graphite anode). All these findings suggest that borophene, as an anode material for Li- or Na-ion batteries, has potential to drastically boost batteries' energy density and power density.

For other two synthesized BSs, β_{12} and χ_3 sheets, both of them were also suggested as potential electrode materials for Li-ion/Na-ion battery,[113] or rechargeable non-lithium-ion batteries (Na^+, K^+, Ca^{2+}, Mg^{2+}, and Al^{3+} NLIBs)[114] as well as lithium-sulfur (Li-S) batteries.[115] The BSs meet all the necessary requirements for a good electrode material: (1) metallic conductivities are maintained before and after Li or Na adsorption; (2) low diffusion barriers of ~0.6 eV, which is larger than that of graphene,[116] MoS_2,[117] but comparable to Silicon or phosphorene,[118] indicating good charge–discharge rates; (3) a very small lattice change (<2.2%) upon Li and Na intercalations, ensuring good cycling stabilities; and (4) most importantly, both β_{12} and χ_3 sheets exhibit extremely high capacity, with 1984 $mAhg^{-1}$ for β_{12} and 1240 $mAhg^{-1}$ for χ_3 sheets, which are several times higher than other typical electrode materials and are the highest among all the 2D material based electrodes studied to date. Nevertheless, all these investigations are based on the theoretical proposal, the experimental demonstrations are urgently required for practical batteries applications.

2D BSs are also suggested to be highly promising electrode materials for supercapacitors due to its unique properties such as excellent electronic conductivity, high specific surface area and low mass density. Zhan et. al[119] chose six 2D BSs (β_{12}, χ_3, α and β sheets) for testing, and demonstrated that they exhibit specific capacitance on the order of 400 F/g, about four times that of graphene, suggesting that 2D BSs are promising electrodes for supercapacitor applications. The inspiring theoretical prediction has been proven from experiments, although the specific measured capacitance is lower, within the range of 91.6 F/g to 142.6 F/g.[57] The BS based supercapacitor exhibits impressive electrochemical performance with a wide potential window of up to 3.0 V, excellent energy density as high as 46.1 Wh/kg at a power density of 478.5 W/kg, and excellent cycling stability with 88.7% retention of the initial specific capacitance after 6000 cycles. The work clearly demonstrated the exfoliated boron materials promising for next generation optoelectronics and energy storage applications.

7. Conclusions and perspectives

As a unique member of 2D family, BSs have been proposed for the decades, however the experimental synthesis was achieved until 2015 due to the structural instability and inherent polymorphism. In the

perspective, we have reviewed the evolution route from planar boron clusters to 2D structures, and theoretical predictions for diverse boron structures, the recent experimental growths of BSs on the substrates, as well as the progress of applications on the energy storages. In the progress of 2D boron research, we can see the importance of theoretical simulations, which can not only provide useful information of stable BSs configurations and the route of practical experimental synthesis, but also help to understand the detailed electronic, mechanical properties.

Even diverse 2D boron structures have been proposed with novel mechanical, electronic and chemical properties, but only a few of them have been confirmed from recent experiments, the researches for the new emerged materials are still in infant period and face great challenges. In details, the challenges can be summarized as 3 prospects. 1) Due to the electron deficiency and absence of naturally layered bulk materials, BS was normally synthesized from chemical growth methods on the substrates, like silver or aluminium,[22, 23, 55] the electron transfer between BS and substrate helps to stabilize the sheets. However, the strong interaction between BSs and substrate leads to the transfer difficulties, namely peering off for other physical experimentations or practical application. The new experimental methods need to be developed for BSs following the successful examples like graphene on Cu (111)[120] or silicene on Ag surface.[121] 2) Compared with inert feature of graphene at ambient environments, the active chemical surface of BSs needs to be protected by capping layers if the intrinsic novel properties will be used. Alternatively, it is necessary to functionalize the surface to increase structural stability and decrease the surface chemical activity. However, precise surface functionalization is still an open research question. 3) Current synthesis of BSs is mainly based on MBE growth, which has the intrinsic disadvantages like limited quantities, and insufficient yield. Although recent studies show that few-layer BSs can be scalable produced by liquid-exfoliation,[57] the methodology deserves further verification since boron does not have a natural 3D allotrope with a layered structure, and therefore micromechanical exfoliation is not suitable for the production of BSs as suggested by the research communities[55] To obtain large scale, quality samples of BSs in a controlled manner, CVD growth is one of the feasible approach[122] despite of numerous unsuccessful attempts.[123]

Despite of these challenges, the researches of BSs are very attractive due to the outstanding physical/chemical properties and great potential for practical applications. Several possible research directions are worthy for the future investigations, 1) the superconductivity from experiments and deep understanding for the mechanism. Different from graphene, the superconductivity of boron sheets are intrinsic, which have been confirmed from different predictions, but be barely experimentally demonstrated. 2) The effects of defects on mechanical, electronic or magnetic properties of boron sheets should be clarified since the vacancies, dislocation or impurities are inevitable during the synthesis. Although recently there is a work on the topic[124], more investigations are required. 3) One of the most important research directions is about the experimental synthesis. Although there are several reports about the fabrications of the sheets as indicated above, most of the proposed systems are waiting for demonstrations. New methodologies are called for. Following the successful synthesis and surface protection techniques as in phosphorene[125] and silicene,[126] these difficulties

are expected to be solved with fast developed cutting-edge nanotechnologies in the near future. The potential applications which fully utilize the novel physics can therefore be achieved with the aid of theoretical tools.

Biography

Jing Shang received her Master degree in Northwestern Polytechnical University (NWPU) in 2016. And now she is a first-year PhD student in Queensland University of Technology (QUT). Her current research interests include mechanical properties of Nickle-based single crystal alloys and electronic properties of two dimensional materials.

Yandong Ma received his B.S. degree in 2009 and Ph.D. in 2014 at Shandong University. Afterwards he worked as a postdoc at Jacobs University. In 2016, he moved to Leipzig University as a postdoc. Since September of 2017, he joined Shandong University as a Full Professor. His research interests focus on the electronic and spintronic behaviors of two-dimensional materials.

Professor Yuantong Gu received his Ph.D. degree in mechanical engineering from National University of Singapore in 2003. After the Postdoc Research Fellow in University of California, Irvine (2004-2005), he was awarded ARC APD fellowship and joined The University of Sydney in 2005. Then, he moved to Queensland

University of Technology since 2007 as a lecturer, and now is a professor and the discipline leader. His research mainly focuses on computational mechanics and its applications in engineering and science.

Dr. Liangzhi Kou received his Ph.D degree from Nanjing University of Aeronautics and Astronautics at 2011. After the Humboldt Fellowship at the Bremen Center of Computational Materials Sciences (2012-2014) and a Research Assistant at UNSW Australia (2014), he was awarded DECRA fellowship from ARC and moved to Queensland University of Technology as a lecturer since 2015, and now is a senior lecturer. His research mainly focuses on computational discovery and design of novel 2D materials for energy applications and 2D topological insulators.

Acknowledgments

We acknowledge the grants of high-performance computer time from computing facility at the Queensland University of Technology, the Pawsey Supercomputing Centre and Australian National Facility. L.K. gratefully acknowledges financial support by the ARC Discovery Early Career Researcher Award (DE150101854). Y.G acknowledges financial support by ARC Discovery grant DP170102861.

References:

1. A. K. Geim, *Science*, 2009, 324, 1530-1534.
2. C. L. Tan, X. H. Cao, X. J. Wu, Q. Y. He, J. Yang, X. Zhang, J. Chen, W. Zhao, S. K. Han, G. H. Nam, M. Sindoro and H. Zhang, *Chem. Rev.*, 2017, 117, 6225-6331.
3. Y. Y. Wen, C. C. Huang, L. Z. Wang and D. H. Jurcakova, *Chin. Sci. Bull.*, 2014, 59, 2102-2121.

4. Y. X. Yu, *Phys. Chem. Chem. Phys.*, 2013, 15, 16819-16827.
5. T. S. Miller, A. B. Jorge, T. M. Suter, A. Sella, F. Cora and P. F. McMillan, *Phys. Chem. Chem. Phys.*, 2017, 19, 15613-15638.
6. Q. H. Weng, X. B. Wang, X. Wang, Y. Bando and D. Golberg, *Chem. Soc. Rev.*, 2016, 45, 3989-4012.
7. M. Pumera, Z. Sofer and A. Ambrosi, *J. Mater. Chem. A*, 2014, 2, 8981-8987.
8. X. Li and H. Zhu, *Journal of Materiomics*, 2015, 1, 33-44.
9. Y. X. Yu, *The J. Phys. Chem. C*, 2016, 120, 5288-5296.
10. Y. Xin and Y.X. Yu, *Mater. Design*, 2017, 130, 512-520.
11. B. Anasori, M. R. Lukatskaya and Y. Gogotsi, *Nat. Rev. Mater.*, 2017, 1, 16098.
12. G. Fiori, F. Bonaccorso, G. Iannaccone, T. Palacios, D. Neumaier, A. Seabaugh, S. K. Banerjee and L. Colombo, *Nat. Nanotechnol.*, 2014, 9, 768-779.
13. S. Zhang, Z. Yan, Y. Li, Z. Chen and H. Zeng, *Angew Chem. Int. Ed. Engl.*, 2015, 54, 3112-3115.
14. S. L. Zhang, F. Y. Li, Z. Yan, Y. F. Li, E. Kan, W. Liu, Z. F. Chen, and H. B. Zeng, *Angew. Chem. Int. Ed.*, 2016, 55, 1666-1669.
15. J. Ji, X. Song, J. Liu, Z. Yan, C. Huo, S. Zhang, M. Su, L. Liao, W. Wang, Z. Ni, Y. Hao and H. Zeng, *Nat. Commun.*, 2016, 7, 13352.
16. S. Zhang, S. Guo, Z. Chen, Y. Wang, H. Gao, J. G. Herrero, P. Ares, F. Zamora, Z. Zhu and H. Zeng, *Chem. Soc. Rev.*, 2018, 47, 982-1021.
17. L. Kou, Y. Ma, X. Tan, T. Frauenheim, A. Du and S. Smith, *J. Phys. Chem. C*, 2015, 119, 6918-6922.
18. A. J. Mannix, B. Kiraly, M. C. Hersam and N. P. Guisinger, *Nat. Rev. Chem.*, 2017, 1, 0014.
19. S. Er, G. A. de Wijs and G. Brocks, *J. Phys.Chem. C*, 2009, 113, 18962-18967.
20. X. J. Wu, J. Dai, Y. Zhao, Z. W. Zhuo, J. L. Yang and X. C. Zeng, *ACS Nono*, 2012, 6, 7443-7453.
21. H. Tang and S. Ismail-Beigi, *Phys. Rev. Lett.*, 2007, 99, 115501.
22. A. J. Mannix, X. F. Zhou, B. Kiraly, J. D. Wood, D. Alducin, B. D. Myers, X. L. Liu, B. L. Fisher, U. Santiago, J. R. Guest, M. J. Yacaman, A. Ponce, A. R. Oganov, M. C. Hersam and N. P. Guisinger, *Science*, 2015, 350, 1513-1516.
23. B. Feng, J. Zhang, Q. Zhong, W. Li, S. Li, H. Li, P. Cheng, S. Meng, L. Chen and K. Wu, *Nat. Chem.*, 2016, 8, 563-568.
24. W. Li, L. Kong, C. Chen, J. Gou, S. Sheng, W. Zhang, H. Li, L. Chen, P. Cheng and K. Wu, *Sci. Bull.*, 2018, 63, 282-286.
25. J. Plesek, *Chem. Rev.*, 1992, 92, 269-278.

26. H. J. Zhai, Y. F. Zhao, W. L. Li, Q. Chen, H. Bai, H. S. Hu, Z. A. Piazza, W. J. Tian, H. G. Lu, Y. B. Wu, Y. W. Mu, G. F. Wei, Z. P. Liu, J. Li, S. D. Li and L. S. Wang, *Nat. Chem.*, 2014, 6, 727-731.
27. Z. J. Lesnikowski, *J. Med. Chem.*, 2016, 59, 7738-7758.
28. A. N. Alexandrova, A. I. Boldyrev, H. J. Zhai and L. S. Wang, *J. Phys. Chem. A*, 2004, 108, 3509-3517.
29. H. J. Zhai, B. Kiran, J. Li and L. S. Wang, *Nat. Mater.*, 2003, 2, 827-833.
30. B. Kiran, S. Bulusu, H. J. Zhai, S. Yoo, X. C. Zeng and L.S. Wang, *PNAS*, 2004, 102, 961-964.
31. Z. A. Piazza, H. S. Hu, W. L. Li, Y. F. Zhao, J. Li and L. S. Wang, *Nat. Commun.*, 2014, 5, 3113.
32. A. B. Rahane and V. Kumar, *Nanoscale*, 2015, 7, 4055-4062.
33. N. G. Szwacki, A. Sadrzadeh and B. I. Yakobson, *Phys. Rev. Lett.*, 2007, 98, 166804.
34. H. Li, N. Shao, B. Shang, L. F. Yuan, J. Yang and X. C. Zeng, *Chem. Commun. (Camb)*, 2010, 46, 3878-3880.
35. L. W. J. J. Zhao, F. Y. Li, and Z. F. Chen, *J. Phys. Chem. A.,* 2010, 114, 9969-9972.
36. F. Li, P. Jin, D. E. Jiang, L. Wang, S. B. Zhang, J. Zhao and Z. Chen, *J. Chem. Phys.*, 2012, 136, 074302.
37. I. Boustani, A. Quandt, E. Hernández and A. Rubio, *J. Chem. Phy.*, 1999, 110, 3176-3185.
38. J. Kunstmann and A. Quandt, *Phys. Rev. B*, 2006, 74, 035413.
39. K. C. L. R. Pandey, *J. Phys. Chem. C*, 2007, 111, 2906-2912.
40. M. H. Evans, J. D. Joannopoulos and S. T. Pantelides, *Phys. Rev. B*, 2005, 72, 045434.
41. E. S. Penev, S. Bhowmick, A. Sadrzadeh and B. I. Yakobson, *Nano Lett.*, 2012, 12, 2441-2445.
42. Z. Zhang, E. S. Penev and B. I. Yakobson, *Chem. Soc. Rev.*, 2017, 46, 6746-6763.
43. W. Choi, I. Lahiri, R. Seelaboyina and Y. S. Kang, *Crit. Rev. Solid State*, 2010, 35, 52-71.
44. L. Kou, C. Chen and S. C. Smith, *J. Phys. Chem. Lett.*, 2015, 6, 2794-2805.
45. L. Z. Zhang, Q. B. Yan, S. X. Du, G. Su and H. J. Gao, *J. Phys. Chem. C*, 2012, 116, 18202-18206.
46. B. Hu, H. Ago, Y. Ito, K. Kawahara, M. Tsuji, E. Magome, K. Sumitani, N. Mizuta, K. Ikeda and S. Mizuno, *Carbon*, 2012, 50, 57-65.
47. Y. Li, M. Li, T. Wang, F. Bai and Y.X. Yu, *Phys. Chem. Chem. Phys.* 2014, 16, 5213.
48. Y. Li, M. Li, T. Gu, F. Bai, Y. Yu, M. Trevor and Y. Yu, *Appl. Surf. Sci.*, 2013, 284, 207-213.
49. Y. Li, M. Li, T. Gu, F. Bai, Y. Yu, T. Mwenya and Y. Yu, *AIP Advances*, 2013, 3, 052130.
50. H. Liu, J. Gao and J. Zhao, *Sci. Rep.*, 2013, 3, 3238.
51. Y. Liu, E. S. Penev and B. I. Yakobson, *Angew Chem. Int. Ed. Engl.*, 2013, 52, 3156-3159.
52. S. Xu, Y. Zhao, J. Liao, X. Yang and H. Xu, *Nano Research*, 2016, 9, 2616-2622.
53. Z. Zhang, Y. Yang, G. Gao and B. I. Yakobson, *Angew Chem. Int. Ed. Engl.*, 2015, 54, 13022-13026.

54. Q. Zhong, J. Zhang, P. Cheng, B. Feng, W. Li, S. Sheng, H. Li, S. Meng, L. Chen and K. Wu, *J. Phys. Condens. Matter.*, 2017, 29, 095002.
55. L. Kong, K. Wu and L. Chen, *Front. Phys.*, 2018, 13, 138105.
56. Z. Zhang, A. J. Mannix, Z. Hu, B. Kiraly, N. P. Guisinger, M. C. Hersam and B. I. Yakobson, *Nano Lett.*, 2016, 16, 6622-6627.
57. H. Li, L. Jing, W. Liu, J. Lin, R. Y. Tay, S. H. Tsang and E. H. T. Teo, *ACS Nano*, 2018, 12, 1262-1272.
58. J. E. Padilha, R. H. Miwa and A. Fazzio, *Phys. Chem. Chem. Phys.*, 2016, 18, 25491-25496.
59. L. C. Xu, A. Du and L. Kou, *Phys. Chem. Chem. Phys.*, 2016, 18, 27284-27289.
60. L. Kou, Y. Ma, C. Tang, Z. Sun, A. Du and C. Chen, *Nano Lett.*, 2016, 16, 7910-7914.
61. B. Feng, J. Zhang, R.Y. Liu, T. Iimori, C. Lian, H. Li, L. Chen, K. Wu, S. Meng, F. Komori and I. Matsuda, *Phys. Rev. B*, 2016, 94, 041408.
62. E. S. Penev, A. Kutana and B. I. Yakobson, *Nano Lett.*, 2016, 16, 2522-2526.
63. B. Feng, O. Sugino, R. Y. Liu, J. Zhang, R. Yukawa, M. Kawamura, T. Iimori, H. Kim, Y. Hasegawa, H. Li, L. Chen, K. Wu, H. Kumigashira, F. Komori, T. C. Chiang, S. Meng and I. Matsuda, *Phys. Rev. Lett.*, 2017, 118, 096401.
64. B. Feng, J. Zhang, S. Ito, M. Arita, C. Cheng, L. Chen, K. Wu, F. Komori, O. Sugino, K. Miyamoto, T. Okuda, S. Meng and I. Matsuda, *Adv. Mater.*, 2018, 30, 1704025.
65. X. F. Zhou, X. Dong, A. R. Oganov, Q. Zhu, Y. Tian and H. T. Wang, *Phys. Rev. Lett.*, 2014, 112, 085502.
66. F. X. Ma, Y. L. Jiao, G. P. Gao, Y. T. Gu, A. Bilic, Z. F. Chen and A. J. Du, *Nano Lett.*, 2016, 16, 3022-3028.
67. H. Zhang, Y. Xie, Z. Zhang, C. Zhong, Y. Li, Z. Chen and Y. Chen, *J. Phys. Chem. Lett.*, 2017, 8, 1707-1713.
68. Y. L. Jiao, F. X. Ma, J. Bell, A. Bilic and A. J. Du, *Angew Chem. Int. Ed. Engl.*, 2016, 55, 10292-10295.
69. L. Z. Zhang, Z. F. Wang, S. X. Du, H. J. Gao and F. Liu, *Phys. Rev. B*, 2014, 90, 161402.
70. B. Z. Xu and S. P. Beckman, *2D Mater.*, 2016, 3, 031003.
71. H. Tang and S. I. Beigi, *Phys. Rev. B*, 2009, 80, 134113.
72. Y. Mu, F. Ding and H. Lu, *RSC Advances*, 2015, 5, 11392-11396.
73. P. Zhang and V. H. Crespi, *Phys. Rev. Lett.*, 2002, 89, 056403.
74. H. Zhang, Y. Li, J. Hou, A. Du and Z. Chen, *Nano Lett.*, 2016, 16, 6124-6129.
75. H. Zhang, Y. Li, J. Hou, K. Tu and Z. Chen, *J. Am. Chem. Soc.*, 2016, 138, 5644-5651.
76. J. H. Yang, S. Song, S. Du, H. J. Gao and B. I. Yakobson, *J. Phys. Chem. Lett.*, 2017, 8, 4594-4599.
77. J. M. An and W. E. Pickett, *Phys. Rev. Lett.*, 2001, 86, 4366-4369.

78. J. Kortus, Mazin, II, K. D. Belashchenko, V. P. Antropov and L. L. Boyer, *Phys. Rev. Lett.*, 2001, 86, 4656-4659.
79. H. J. Choi, D. Roundy, H. Sun, M. L. Cohen and S. G. Louie, *Nat. Rev. Chem.*, 2002, 418, 758-760.
80. Y. C. Zhao, S. M. Zeng and J. Ni, *Phys. Rev. B*, 2016, 93, 014502.
81. Y. Zhao, S. Zeng and J. Ni, *Appl. Phys. Lett.*, 2016, 108, 242601.
82. M. Gao, Q. Z. Li, X. W. Yan and J. Wang, *Phys. Rev. B*, 2017, 95, 024505.
83. G. Profeta, M. Calandra and F. Mauri, *Nat. Phys.*, 2012, 8, 131-134.
84. M. Xue, G. Chen, H. Yang, Y. Zhu, D. Wang, J. He and T. Cao, *J. Am. Chem. Soc.*, 2012, 134, 6536-6539.
85. C. Cheng, J. T. Sun, H. Liu, H. X. Fu, J. Zhang, X. R. Chen and S. Meng, *2D Materials*, 2017, 4, 025032.
86. R. C. Xiao, D. F. Shao, W. J. Lu, H. Y. Lv, J. Y. Li and Y. P. Sun, *Appl. Phys. Lett.*, 2016, 109, 122604.
87. C. Wu, H. Wang, J. Zhang, G. Gou, B. Pan and J. Li, *ACS Appl. Mater. Interface.*, 2016, 8, 2526-2532.
88. B. Mortazavi, O. Rahaman, A. Dianat and T. Rabczuk, *Phys. Chem. Chem. Phys.*, 2016, 18, 27405-27413.
89. C. G. Lee, X. D. Wei, J. W. Kysar and J. Hone, *Science*, 2008, 321, 385-388.
90. Z. Zhang, Y. Yang, E. S. Penev and B. I. Yakobson, *Adv. Funct. Mater.*, 2017, 27, 1605059.
91. L. Adamska, S. Sadasivam, J. J. Foley, P. Darancet and S. Sharifzadeh, *The J. Phys. Chem. C*, 2018, 122, 4037-4045.
92. W. W. Luo, G. Liu, X. Wang, X. L. Lei, C. Y. Ouyang and S. Q. Liu, *Physica B: Condensed Matter.*, 2018, 537, 1-6.
93. J. Xu, Y. Chang, L. Gan, Y. Ma and T. Zhai, *Adv. Sci. (Weinh)*, 2015, 2, 1500023.
94. X. Tang, A. Du and L. Kou, *Wiley Interdiscip. Rev.: Comput. Mol. Sci.*, 2018, 8, e1361.
95. V. Tozzini and V. Pellegrini, *Phys. Chem. Chem. Phys.*, 2013, 15, 80-89.
96. D. B. Putungan, S. H. Lin, C. M. Wei and J. L. Kuo, *Phys. Chem. Chem. Phys.*, 2015, 17, 11367-11374.
97. P. Banerjee, B. Pathak, R. Ahuja and G. P. Das, *Int. J. Hydrogen Energ.*, 2016, 41, 14437-14446.
98. A. M. Seayad and D. M. Antonelli, *Adv. Mater.*, 2004, 16, 765-777.
99. C. Ataca, E. Aktürk and S. Ciraci, *Phys. Rev. B*, 2009, 79, 041406.
100. X. Tang, Y. Gu and L. Kou, *Chem. Phys. Lett.*, 2018, 695, 211-215.
101. X. Chen, L. Wang, W. Zhang, J. Zhang and Y. Yuan, *Int. J. Hydrogen Energ.*, 2017, 42, 20036-20045.
102. L. Li, H. Zhang and X. Cheng, *Comput. Mater. Sci.*, 2017, 137, 119-124.

103. Y. Ji, H. Dong and Y. Li, *ChemistrySelect*, 2017, 2, 10304-10309.
104. L. Wang, X. Chen, H. Du, Y. Yuan, H. Qu and M. Zou, *Appl. Surf. Sci.*, 2018, 427, 1030-1037.
105. M. Li, Y. F. Li. Z. Zhou, P. W. Shen, and Z. F. Chen, *Nano Lett.*, 2009, 9, 1944-1948
106. H. R. Jiang, Z. Lu, M. C. Wu, F. Ciucci and T. S. Zhao, *Nano Energy*, 2016, 23, 97-104.
107. Y. Zhang, Z. F. Wu, P. F. Gao, S. L. Zhang and Y. H. Wen, *ACS Appl. Mater. Interface.*, 2016, 8, 22175-22181.
108. B. Mortazavi, A. Dianat, O. Rahaman, G. Cuniberti and T. Rabczuk, *J. Power Sources*, 2016, 329, 456-461.
109. D. Rao, L. Zhang, Z. Meng, X. Zhang, Y. Wang, G. Qiao, X. Shen, H. Xia, J. Liu and R. Lu, *J. Mater. Chem. A*, 2017, 5, 2328-2338.
110. P. Liang, Y. Cao, B. Tai, L. Zhang, H. Shu, F. Li, D. Chao and X. Du, *J. Alloy Comp.*, 2017, 704, 152-159.
111. B. Mortazavi, O. Rahaman, S. Ahzi and T. Rabczuk, *Appl. Mater. Today*, 2017, 8, 60-67.
112. N. K. Jena, R. B. Araujo, V. Shukla and R. Ahuja, *ACS Appl. Mater. Interfaces*, 2017, 9, 16148-16158.
113. X. Zhang, J. Hu, Y. Cheng, H. Y. Yang, Y. Yao and S. A. Yang, *Nanoscale*, 2016, 8, 15340-15347.
114. P. Xiang, X. Chen, W. Zhang, J. Li, B. Xiao, L. Li and K. Deng, *Phys. Chem. Chem. Phys.*, 2017, 19, 24945-24954.
115. L. Zhang, P. Liang, H. B. Shu, X. L. Man, F. Li, J. Huang, Q. M. Dong and D. L. Chao, *J. Phys. Chem. C*, 2017, 121, 15549-15555.
116. E. Pollak, B. Geng, K. J. Jeon, I. T. Lucas, T. J. Richardson, F. Wang and R. Kostecki, *Nano Lett.*, 2010, 10, 3386-3388.
117. L. David, R. Bhandavat and G. Singh, *ACS Nano*, 2014, 8, 1759-1770.
118. S. Zhao, W. Kang and J. Xue, *J. Mater. Chem. A*, 2014, 2, 19046-19052.
119. C. Zhan, P. Zhang, S. Dai and D. E. Jiang, *ACS Energy Lett.*, 2016, 1, 1241-1246.
120. X. S. Li, W. W. Cai, J. An, S. Kim, J. Nah, D. X. Yang, R. Piner, A. Velamakanni, I. Jung, E. Tutuc, S. K. Banerjee, L Colombo and R. S. Ruoff, *Science*, 2009, 324, 1312.
121. P. Vogt, P. De Padova, C. Quaresima, J. Avila, E. Frantzeskakis, M. C. Asensio, A. Resta, B. Ealet and G. Le Lay, *Phys. Rev. Lett.*, 2012, 108, 155501.
122. G. A. Tai, T.S. Hu, Y. G. Zhou, X. F. Wang, J. Z. Kong, T. Zeng, Y. C. You and Q. Wang, *Angew. Chem. Int. Ed.*, 2015, 54, 15473-15477.
123. B. J. Bellott, W. Noh, R. G. Nuzzo and G. S. Girolami, *Chem. Commun. (Camb)*, 2009, 3214-3215.
124. X. Liu, Z. Zhang, L. Wang, B. I. Yakobson and M. C. Hersam, *Nat. Mater.*, 2018, 17, 783-788.
125. H. S. Ra, A. Y. Lee, D. H. Kwak, M. H. Jeong and J. S. Lee, *ACS Appl. Mater. Interfaces*, 2018, 10, 925-932.

126. L. Tao, E. Cinquanta, D. Chiappe, C. Grazianetti, M. Fanciulli, M. Dubey, A. Molle and D. Akinwande, *Nat Nanotechnol.*, 2015, 10, 227-231.